

See discussions, stats, and author profiles for this publication at: <https://www.researchgate.net/publication/231235986>

# Molecular Templating of Nanoporous Ultralow Dielectric Constant ( $\approx 1.5$ ) Organosilicates by Tailoring the Microphase Separation of Triblock Copolymers

ARTICLE in CHEMISTRY OF MATERIALS · AUGUST 2001

Impact Factor: 8.35 · DOI: 10.1021/cm0102786

CITATIONS

85

READS

21

9 AUTHORS, INCLUDING:



Shu Yang

University of Pennsylvania

207 PUBLICATIONS 5,144 CITATIONS

SEE PROFILE



Eric Lin

National Institute of Standards and Technolo...

223 PUBLICATIONS 3,955 CITATIONS

SEE PROFILE



Hae-Jeong Lee

National Institute of Standards and Technolo...

72 PUBLICATIONS 967 CITATIONS

SEE PROFILE



David W. Gidley

University of Michigan

183 PUBLICATIONS 4,246 CITATIONS

SEE PROFILE

# Molecular Templating of Nanoporous Ultralow Dielectric Constant ( $\approx 1.5$ ) Organosilicates by Tailoring the Microphase Separation of Triblock Copolymers

Shu Yang,<sup>\*,†</sup> Peter A. Mirau,<sup>†</sup> Chien-Shing Pai,<sup>†</sup> Omkaram Nalamasu,<sup>†</sup> Elsa Reichmanis,<sup>†</sup> Eric K. Lin,<sup>‡</sup> Hae-Jeong Lee,<sup>‡</sup> David W. Gidley,<sup>§</sup> and Jianing Sun<sup>||</sup>

Bell Laboratories, Lucent Technologies,  
600 Mountain Avenue,  
Murray Hill, New Jersey 07974, National Institute of  
Standards and Technology, Polymers Division,  
100 Bureau Drive,  
Gaithersburg, Maryland 20899-8541, and  
Departments of Physics and Materials Science and  
Engineering, University of Michigan,  
Ann Arbor, Michigan 48109

Received March 29, 2001

Revised Manuscript Received July 18, 2001

Porous materials have uses in many potential applications including membranes, sensors, waveguides, dielectrics, and microfluidic channels.<sup>1–5</sup> These materials have attracted tremendous interest in the microelectronics industry as a means of fabricating low dielectric constant films.<sup>6</sup> When the packing density between multilevel interconnects increases, a low dielectric constant material is needed to replace the current wire insulator, silicon dioxide ( $k \approx 4.0$ ) to minimize RC delay. However, most solid materials have  $k > 3$ . As a result, voids are introduced into the film by taking advantage of the low dielectric constant of air ( $k = 1$ ) to achieve ultralow  $k$  ( $k \leq 2.2$ ). Meanwhile, the pore size, shape, and distribution strongly affect thin film properties. Although many types of porous materials have been explored in past years, few meet the stringent requirements for ultralow  $k$  materials, namely, good thermal stability (above 400 °C), low moisture uptake, high mechanical strength, and dielectric breakdown field.

Porous silica with ordered structures as ultralow  $k$  materials have been fabricated through sol–gel processes.<sup>3,4</sup> However, the high porosity (>50%) required in this approach raises concerns about the mechanical stability of the resultant materials. Moreover, subse-

quent surface treatment and film aging must be applied to minimize moisture absorption. Hydrophobic organosilicates, such as poly(methyl silsesquioxane) (MSQ), are also promising matrix materials for ultralow  $k$  dielectrics. MSQ has a relatively low dielectric constant ( $k \approx 2.6$ – $2.8$ ) and minimal moisture absorption. For example, IBM researchers have used hyperbranched poly( $\epsilon$ -caprolactone) (PCL) as porogens to generate porous MSQ.<sup>5,7</sup> In contrast to the silica, MSQ-based organosilicates change their nature substantially from amphiphilic to hydrophobic during curing, altering the miscibility of a given template material in solution and during curing.<sup>8</sup> A good match between the polymer template and MSQ matrix both before and after curing is critical for control over the final pore structure and film properties. However, the phase behavior of the nanocomposite organosilicates in solution or in a thin film is not well understood.

Block copolymers are good candidate materials for templates because they can microphase separate into nanometer-scale domains.<sup>9</sup> Recently, they have been used as templates to fabricate bulk mesoporous inorganic and organic/inorganic hybrids with a variety of morphologies.<sup>10–13</sup>

Here, we use triblock copolymers, poly(ethylene oxide-*b*-propylene oxide-*b*-ethylene oxide) (PEO-*b*-PPO-*b*-PEO), as sacrificial templates in a poly(methyl silsesquioxane) matrix (see Scheme 1). The amphiphilic triblock copolymers are known as polymeric surfactants, which associate into micelles with PEO shells in aqueous solutions.<sup>8,11,14</sup> More importantly, both blocks have very low glass transition temperatures ( $T_g$ 's), ca.  $-70$  °C, which allow the polymer chains to rapidly self-organize in the matrix during the curing process.

First, Pluronic F88 or P103 (from BASF<sup>15</sup>) was dissolved in *n*-butanol and mixed with a MSQ precursor (from Techneglass<sup>15</sup> as a solution with a mass fraction of 30% in *n*-butanol). F88 and P103 have relative molecular masses of 11400 and 4950 g/mol and PEO mass fractions of 80 and 30%, respectively. The MSQ precursor has a  $M_{r,n}$  of 1668 and polydispersity of 3.2 measured by GPC. <sup>29</sup>Si NMR shows that it has two characteristic signals of T<sub>2</sub> and T<sub>3</sub>, with a ratio of 50:50. Two-dimensional solution-state nuclear Overhauser

\* To whom correspondence should be addressed.

† Lucent Technologies.

‡ National Institute of Standards and Technology.

§ Department of Physics, University of Michigan.

|| Department of Materials Science and Engineering, University of Michigan.

(1) Boyle, T. J.; Brinker, C. J.; Gardner, T. J.; Sault, A. G.; Hughes, R. C. *Comments Inorganic Chem.* **1999**, *20*, 209.

(2) Huo, Q. S.; Zhao, D. Y.; Feng, J. L.; Weston, K.; Buratto, S. K.; Stucky, G. D.; Schacht, S.; Schuth, F. *Adv. Mater.* **1998**, *9*, 974.

(3) Baskaran, S.; Liu, J.; Domansky, K.; Kohler, N.; Li, X. H.; Coyle, C.; Fryxell, G. E.; Thevuthasan, S.; Williford, R. E. *Adv. Mater.* **2000**, *12*, 291.

(4) Lu, Y. F.; Fan, H. Y.; Doke, N.; Loy, D. A.; Assink, R. A.; LaVan, D. A.; Brinker, C. J. *J. Am. Chem. Soc.* **2000**, *122*, 5258.

(5) Hedrick, J. L.; Miller, R. D.; Hawker, C. J.; Carter, K. R.; Volksen, W.; Yoon, D. Y.; Trollsas, M. *Adv. Mater.* **1998**, *10*, 1049.

(6) Miller, R. D. *Science* **1999**, *286*, 421.

(7) Nguyen, C. V.; Carter, K. R.; Hawker, C. J.; Hedrick, J. L.; Jaffe, R. L.; Miller, R. D.; Remenar, J. F.; Rhee, H.-W.; Rice, P. M.; Toney, M. F.; Trollsas, M.; Yoon, D. Y. *Chem. Mater.* **1999**, *11*, 3080.

(8) Alexandridis, P.; Holzwarth, J. F.; Hatton, T. A. *Macromolecules* **1994**, *27*, 2414.

(9) Hamley, I. W. *The Physics of Block Copolymers*; Oxford University Press: Oxford, 1998.

(10) Templin, M.; Franck, A.; DuChesne, A.; Leist, H.; Zhang, Y. M.; Ulrich, R.; Schädler, V.; Wiesner, U. *Science* **1997**, *278*, 1795.

(11) Yang, P. D.; Zhao, D. Y.; Chmelka, B. F.; Stucky, G. D. *Chem. Mater.* **1998**, *10*, 2033.

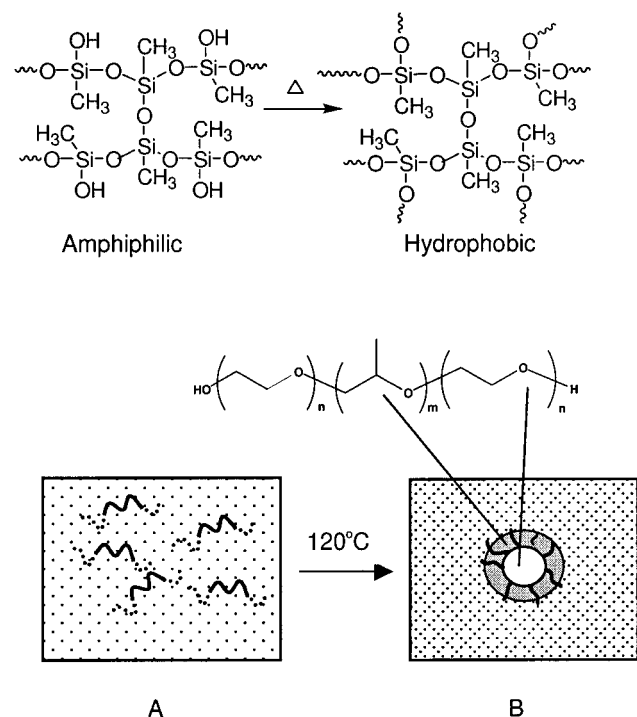
(12) Zhao, D. Y.; Huo, Q. S.; Feng, J.; Melosh, N.; Fredrickson, G. H.; Chmelka, B. F.; Stucky, G. D. *Science* **1998**, *279*, 548.

(13) Chan, V. Z.-H.; Hoffman, J.; Lee, V. Y.; Iatrou, H.; Avgeropoulos, A.; Hadjichristidis, N.; Miller, R. D.; Thomas, E. L. *Science* **1999**, *286*, 1716.

(14) Schmolka, I. R. *J. Am. Oil Chem. Soc.* **1977**, *54*, 110.

(15) Certain commercial equipment and materials are identified in this paper to specify adequately the experimental procedure. In no case does such identification imply recommendation by the National Institute of Standards and Technology nor does it imply that the material or equipment is necessarily the best available for this purpose.

**Scheme 1. Schematic Structures of Phase Behaviors of PEO-*b*-PPO-*b*-PEO Triblock Copolymers in MSQ Matrixes: (A) In the Solution before Curing; (B) in the Thin Film after Curing at 120 °C for 12 h**



effect spectroscopy<sup>16</sup> data from these solutions show that the polymer has a random coil structure and that there is no strong polymer–MSQ interaction.<sup>17</sup> The solution was then spun onto (100) Si wafers, followed by baking and curing steps to lock the polymer into the MSQ matrix.

The polymer domain size and the polymer–MSQ interaction define the final pore size and structure. Here, we have used solid-state proton NMR with and without fast magic-angle sample spinning to probe the self-assembly process of the nanocomposite and to determine the polymer domain size in the thin film.<sup>29</sup> Si NMR data show that, during the polycondensation of the MSQ precursor at 120 °C, the surface of the MSQ becomes hydrophobic. Further, high-resolution <sup>1</sup>H NMR spectra from fast magic-angle spinning and 2-D spin-exchange NMR<sup>18</sup> show that the PPO block is next to the MSQ interface, while the hydrophilic PEO block is buried inside, away from contact with the hydrophobic matrix.<sup>19</sup> This suggests that a reverse micelle is formed in parallel with the change of the MSQ from amphiphilic to hydrophobic during heating (see Scheme 1). This structure facilitates miscibility between the triblock copolymers and the MSQ in the film.

A dipolar filter pulse sequence followed by a spin diffusion delay time<sup>20</sup> has been used to probe the molecular dynamics of the composites and to measure the length scale of phase separation.<sup>21,22</sup> This procedure

**Table 1. Comparison of Polymer Domain Size in the F88/MSQ Composites with Different Polymer Loadings to the Average Pore Sizes Measured by SANS and PALS; A Similar Trend Is Observed in the P103/MSQ System<sup>a,b</sup>**

polymer loadings mass fractions (%)	15	30	40	50
<i>k</i>	2.34	2.0	1.75	1.5
<i>d</i> (nm)	3.7	7.2	7.5	10.3
<i>d<sub>p</sub></i> (nm)	6.2	12.5	11.3	13.9
porosity (%)	N/A	24 ± 9	45 ± 6	53 ± 6
average chord length (nm) (SANS)	N/A	1.4 ± 0.3	3.5 ± 0.4	5.2 ± 0.7
pore size (nm) (PALS)	2.2 ± 0.2	2.7 ± 0.2	4.5 ± 0.3	4.8 ± 0.3

<sup>a</sup> In our solid-state NMR measurements, we use the same dimensionality derived from PALS to calculate *d* and *d<sub>p</sub>*. At a mass fraction of 15%, a three-dimensional cubic pore model is used to fit the data. When the F88 mass fraction is above 30%, a two-dimensional tubular pore model is used. <sup>b</sup> The samples for NMR measurement are cured at 120 °C, a partially cured condition. The pore size measured by SANS and PALS are from samples treated at 500 °C.

can be used to estimate the distance *d* across the minor phase and the overall repeat distance, or long period *d<sub>p</sub>*. For a nanocomposite with an F88 mass fraction of 15%, *d* and *d<sub>p</sub>* are 3.7 and 6.2 nm, respectively.<sup>23</sup> In comparison, the bulk F88 has a PPO domain size of 6.1 nm and a long period of 8.8 nm. Furthermore, it is found that the PEO block is predominantly crystalline in the bulk copolymer, while both the PPO and PEO blocks are mobile in the MSQ nanocomposite, allowing them to form a dense core–shell structure as the matrix cures (Scheme 1). This suggests that microphase separation between PEO and PPO greatly affects how the polymers organize in the matrix. The polymer loading controls the polymer domain size in the composite (see Table 1).

After pores were generated by heating the nanocomposites above 400 °C under N<sub>2</sub>, *k* (*f* = 1 kHz) decreased from 2.6–2.8 to 1.5 with a block copolymer mass fraction of 50% (see Table 1). Although *k* depends mainly on the film porosity, large and open pores could make the film more susceptible to metal diffusion and adversely affect the electrical or mechanical properties and adhesion.

Current–voltage curves were measured for different porous MSQ films (Figure 1). All the porous MSQ films show a very high breakdown field (>2 MV/cm) and a Young's modulus of ≈3 GPa at polymer mass fractions of 30%. Fused glass (≈58 GPa) was used as a reference. Films with *k* ≈ 1.5 do not collapse and have a Young's modulus of ≈0.6 GPa. Recent XPS data show no copper diffusion through an industrial standard thin diffusion barrier, TaN, when annealed at 500 °C for 4 h. This is the first demonstration of a record-low dielectric constant, ≈1.5, with both electrical and mechanical integrity because of small pores in thin films.

The pore size and structure of the film were measured nondestructively by a combination of X-ray reflectivity and small-angle neutron scattering (XR/SANS)<sup>24</sup> and

(16) Jeneer, J.; Meier, B.; Bachmann, P.; Ernst, R. *J. Chem. Phys.* **1979**, *71*, 4546.

(17) Mirau, P. A.; Bovey, F. *Macromolecules* **1990**, *23*, 4548.

(18) Mirau, P. A.; Heffner, S. A. *Macromolecules* **1999**, *32*, 4912.

(19) Mirau, P. A.; Yang, S., unpublished data.

(20) Egger, N.; Schmidtrohr, K.; Blumich, B.; Domke, W. D.; Stapp, B. *J. Appl. Polym. Sci.* **1992**, *44*, 289.

(21) Clauss, J.; Schmidtrohr, K.; Spiess, H. W. *Acta Polym.* **1993**, *44*, 1.

(22) VanderHart, D. L.; McFadden, G. B. *Solid State Nucl. Magn. Reson.* **1996**, *7*, 45.

(23) The domain sizes were measured in static samples using 10 cycles of the dipolar filter with a 20-μs delay between pulses to saturate the signals from the MSQ. The domain sizes were measured using established procedures.<sup>22</sup> The spin diffusion coefficients were measured from the static spin–spin relaxation times.<sup>27</sup>

(24) Wu, W. L.; Wallace, W. E.; Lin, E. K.; Lynn, G. W.; Glinka, C. *J. J. Appl. Phys.* **2000**, *87*, 1193.

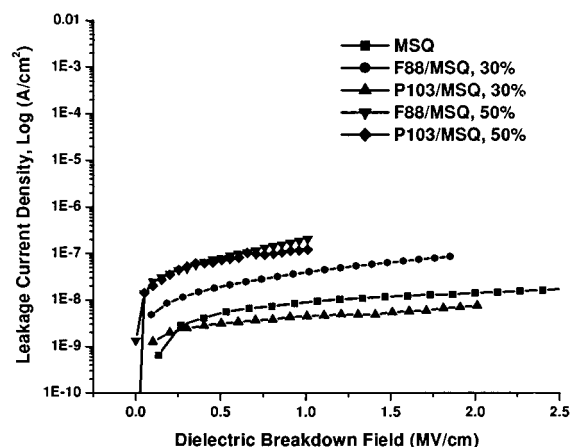


**Figure 1.** Dielectrical breakdown strength of ultralow  $k$  materials with different polymer mass fractions. The applied voltage is ramped from 0 to 100 V at a step of 5 V/s.

positronium annihilation lifetime spectroscopy (PALS).<sup>25</sup> These techniques more quantitatively measure the porosity and average pore size of these films as processed on the silicon wafer than cross-sectional TEM.

Single-crystal silicon wafers are essentially transparent to neutrons and scattering arises primarily from the pore structure. With fitting of the SANS data with the random two-phase Debye model, assuming that the film has the elemental composition of the cured MSQ resin, and measuring of the average film density from XR, the pore size, porosity, density of the overall dielectric film, and pore wall density are determined. For example, the porous MSQ with an F88 mass fraction of 30% has an overall density and a wall density of  $0.88 \pm 0.02$  and  $1.16 \pm 0.16$  g/cm<sup>3</sup>, respectively. The pore size (the average chord length of the two-phase material) is found to be extremely small,  $1.4 \pm 0.3$  nm, and the film porosity is  $24 \pm 9\%$  (see Table 1).<sup>26</sup>

These small pore sizes are close to the limit of SANS probing capability; however, they are well within the

sensitivity of PALS. When positronium (Ps) is formed within an insulator, it tends to localize in open-volume pores. The reduced Ps annihilation lifetime is associated with the average pore size as measured by its mean free path (mathematically identical to the average chord length). The pore interconnectivity (open vs closed) can be deduced from the intensity and lifetime of Ps that can diffuse through the film and escape into vacuum. When interconnected pores are detected, an 80-nm silica cap is deposited to confine Ps to the pores in the film. For interconnected pores, a two-dimensional tubular pore model is used, while for isolated pores a three-dimensional cubic pore model is used to fit the data. At an F88 mass fraction of 30%, the pores have an average pore size of  $2.7 \pm 0.2$  nm. This value correlates well with the pore size obtained from SANS and is consistent with the domain size of the polymer template measured by solid-state NMR. At an F88 mass fraction of 50%, the pore sizes are still small,  $5.2 \pm 0.7$  nm from SANS and  $4.8 \pm 0.3$  nm from PALS measurements.

The templating method reported here provides a simple and straightforward approach to achieve superior electrical and mechanical properties in porous materials with a record-low dielectric constant,  $\approx 1.5$ . The unique characteristics of triblock copolymers allow one to tailor the miscibility and size of nanostructured domains to match changes in the matrix material. A molecular level understanding of the self-assembly mechanism of hybrid materials is essential to the design of nanoporous materials for ultralow  $k$  and other potential applications.

**Acknowledgment.** We would like to thank Janice C. Pai for some sample preparation and dielectric constant measurements. Andy Lovinger is acknowledged for top-view TEM study, Yaw Obeng is acknowledged for nanoindentation measurement, and Robert Opila is acknowledged for XPS study. We are grateful to Pierre Wiltzius for helpful discussion. We finally acknowledge the support of NIST, the U. S. Department of Commerce, and the National Science Foundation, through Agreements DMR-9423101 and ECS-9732804, in providing neutron and positron research facilities, respectively, for this work.

CM0102786

(25) Gidley, D. W.; Frieze, W. E.; Dull, T. L.; Sun, J.; Yee, A. F.; Nguyen, C. V.; Yoon, D. Y. *Appl. Phys. Lett.* **2000**, *76*, 1282.

(26) These data from SXR and SANS are presented with the standard uncertainty of the measurements.

(27) Mellinger, F.; Wilhelm, M.; Spiess, H. *Macromolecules* **1999**, *32*, 4686.